The m^{6}A reader YTHDC2 is essential for escape from KSHV SOX-induced RNA decay

Daniel Macveigh-Fierro[a,b], Angelina Cicerchia[a], Ashley Cadorette[a], Vasudha Sharma[a], and Mandy Muller[a,b,1]

[a]Department of Microbiology, University of Massachusetts, Amherst, MA 01003; and [b]Molecular and Cellular Biology Graduate Program, University of Massachusetts, Amherst, MA 01003

Edited by Bernard Moss, Laboratory of Viral Diseases, National Institute of Allergy and Infectious Diseases, Bethesda, MD; received September 9, 2021; accepted January 13, 2022

The role of N6-methyladenosine (m^{6}A) modifications has increasingly been associated with a diverse set of roles in modulating viruses and influencing the outcomes of viral infection. Here, we report that the landscape of m^{6}A deposition is drastically shifted during Kaposi's sarcoma–associated herpesvirus (KSHV) lytic infection for both viral and host transcripts. In line with previous reports, we also saw an overall decrease in host methylation in favor of viral messenger RNA (mRNA), along with 5′ hypomethylation and 3′ hypermethylation. During KSHV lytic infection, a major shift in overall mRNA abundance is driven by the viral endoribonuclease SOX, which induces the decay of greater than 70% of transcripts. Here, we reveal that interlukin-6 (IL-6) mRNA, a well-characterized, SOX-resistant transcript, is m^{6}A modified during lytic infection. Furthermore, we show that this modification falls within the IL-6 SOX resistance element, an RNA element in the IL-6 3′ untranslated region (UTR) that was previously shown to be sufficient for protection from SOX cleavage. We show that the presence of this m^{6}A modification is essential to confer SOX resistance to the IL-6 mRNA. We next show that this modification recruits the m^{6}A reader YTHDC2 and found that YTHDC2 is necessary for the escape of the IL-6 transcript. These results shed light on how the host cell has evolved to use RNA modifications to circumvent viral manipulation of RNA fate during KSHV infection.

herpesvirus | RNA decay | m^{6}A | m^{6}A readers | IL-6

DNA and RNA viruses regulate the transcriptional and posttranscriptional fate of host messenger RNA (mRNA) to gain access to key resources during infection. Many diverse viruses, including the gammaherpesvirus, Kaposi's sarcoma–associated herpesvirus (KSHV), trigger a widespread mRNA decay event known as "host shutoff" that decimates greater than 70% of the cellular transcriptome (1–5). To achieve this level of degradation, KSHV encodes ORF37 (SOX), an endoribonuclease conserved throughout the gammaherpesvirus family. SOX is responsible for host shutoff, using RNA degradation to dampen cellular gene expression and any mounting immune responses (1, 5, 6), allowing the virus access to newly freed host resources for viral replication. SOX is known to internally cleave cytoplasmic mRNAs in a site-specific manner which then promotes degradation by the cellular 5′ to 3′ exonuclease Xrn1 (7–9). However, over the past decade, we and others have found select mRNA transcripts that robustly escape SOX-induced decay (10, 11). Multiple mechanisms have been hypothesized to explain what contributes to promoting escape from SOX, ranging from a lack of a SOX-targeting motif to indirect transcriptional effects (12, 13). More recently, we have demonstrated that there is a smaller subset of cellular transcripts that actively evade SOX. These "dominant" escapees each carry a specific RNA element found within their 3′ untranslated regions (UTRs) termed the SOX resistance element (SRE). The SRE confers protection to the target transcript from SOX even if the transcript contains an SOX-targeting motif (10, 14, 15). Interestingly, the SRE can resist multiple viral endonucleases but not cellular endonucleases, making it a virus-specific RNase escape element (15, 16).

To date, it is still unknown how many of these SREs are present in the genome, their mechanism of action against viral endonucleases, or what becomes of the SRE-containing transcripts once they are spared from degradation. So far, three SRE-containing "escapees" have been identified: interleukin-6 (IL-6), growth arrest DNA damage-inducible 45 beta (GADD45B), and C19ORF66 (10, 14–17). Although there is little sequence homology among known SREs, they share similarities in their secondary structures, bolstering the idea that the SRE may act as a platform for the recruitment of a protective protein complex (15, 16). Furthermore, it was observed that the SRE is only active when located in the 3′ UTR region of a transcript, suggesting that this RNA element likely functions in conjunction with proteins to modulate RNA stability (14, 15). Previous mass spectrometry screens have identified several host proteins that can bind to the SRE, and intriguingly, a few of these proteins are N^6-methyladenosine (m^{6}A) readers (15).

m^{6}A is the most prevalent mRNA modification out of the over hundred different known RNA modifications (18, 19). m^{6}A impacts virtually every stage of posttranscriptional mRNA fate from splicing, localization, translation, and decay (20–24). Deposition of m^{6}A occurs co- or posttranscriptionally via an m^{6}A writer complex that consists of a catalytic methyltransferase subunit, such as METTL3, and other cofactors, such as

Significance

N6-methyladenosine (m^{6}A) modifications play important roles in regulating RNA fate, in particular during viral infection. However, it remains unclear whether m^{6}A modifications can also act in any antiviral capacity. During Kaposi's sarcoma–associated herpesvirus infection, while most messenger RNA are degraded by the viral nuclease SOX, a subset of transcripts stringently escape degradation. Our study reveals that one such transcript, interleukin-6, acquires an m^{6}A modification during the course of infection, which allows it to recruit the m^{6}A reader YTHDC2. We show that this m^{6}A modification along with the concomitant recruitment of YTHDC2 is essential to provide protection from SOX-induced decay. This suggests that m^{6}A modifications can contribute to the host efforts to regain control of the gene expression environment.

Author contributions: D.M.-F. and M.M. designed research; D.M.-F., A. Cicerchia, A. Cadorette, and V.S. performed research; D.M.-F. analyzed data; and D.M.-F. and M.M. wrote the paper.

The authors declare no competing interest.

This article is a PNAS Direct Submission.

[1]To whom correspondence may be addressed. Email: mandymuller@umass.edu.

This article contains supporting information online at http://www.pnas.org/lookup/suppl/doi:10.1073/pnas.2116662119/-/DCSupplemental.

Published February 17, 2022.

METTL14/16 and WTAP (25–29). The writer complex recognizes a DRACH (D = G/A/U, R = G/A, H = A/U/C) motif for methylation. Although a transcript can have several DRACH motifs, not all will be methylated (25). What determines which motif will be chosen is still unknown (30, 31). Demethylases or erasers like FTO and ALKBH5 add a layer of reversibility to the m^{6}A epitranscriptome (32, 33). The presence or absence of these modifications can change the secondary structure of mRNA and create platforms for m^{6}A reader proteins. Reader proteins then recognize the modification and promote specific RNA fates in turn (21, 25–29, 34).

Recent transcriptome-wide m^{6}A mapping of multiple viruses (35–40) have been brought to the forefront research concerning a complex interplay between the m^{6}A pathways and viral replication success. Previous research has shown that KSHV can hijack this system to deposit m^{6}A onto its own transcripts, including KSHV ORF50 (RTA), the master latent-to-lytic switch protein, and on the multifunction long-noncoding RNA (lncRNA) PAN (36, 41–43). While there is strong evidence that the m^{6}A landscape is reshaped during KSHV infection, and that these shifts ultimately promote the progression of KSHV infection, it remains unclear whether this m^{6}A repurposing also affects the fate of host transcripts.

Here, we show that the IL-6 mRNA is m^{6}A modified in its 3′ UTR during KSHV lytic infection and that removal of this m^{6}A mark restores susceptibility to SOX-mediated degradation. We further show that the m^{6}A reader YTHDC2 binds to the IL-6 SRE in an m^{6}A-dependent manner and that downregulation of YTHDC2 is sufficient to abrogate resistance to SOX. Taken together, these results demonstrate that the m^{6}A pathway is pivotal in the regulation of gene expression during KSHV infection, highlighting the viral–host battle for control of RNA stability.

Results

KSHV Infection Reshapes the m6A Landscape in Cells. Since KSHV reactivation broadly affects RNA fate and extensively remodels the host gene expression environment, we hypothesized that m^{6}A modifications may be broadly redistributed upon KSHV lytic reactivation from latency. We mapped transcriptome-wide m^{6}A modification sites with single-nucleotide resolution using m^{6}A-eCLIP. RNA was isolated from KSHV-positive iSLK.219 cells either in their latent state (Lat) or lytic state (Lyt) 48-h postreactivation and an anti-m^{6}A antibody was used to enrich m^{6}A-modified RNA fragments prior to RNA sequencing of both the input and immunoprecipitated (IP) samples (Fig. 1*A* and Tables S1 and S2). The ratio of IP and input reads were evaluated in each cluster, and clusters with IP/input enrichment greater than eightfold and associated P value < 0.001 were defined as significant "peaks." We detected a total of 2,281 peaks in the latent samples and 1,482 peaks in the reactivated samples. A tool called PureCLIP was used on these peaks to then identify over 40,000 unique, single-nucleotide–resolved sites, which 54% of sites were identical in both of our samples. As expected, the m^{6}A motif DRACH (in particular, [GGACU]) was enriched under the identified peaks, confirming that our m^{6}A deposition in these infected cells is concordant with previous observations (Fig. 1*B*) (35, 36). Also, in agreement with previous data, m^{6}A peaks were most prevalent around the transcript STOP codon and beginning of the 3′ UTR (Fig. 1*C*). The overall m^{6}A peak deposition profiles between Lat and Lyt samples were surprisingly close; however, we observed decreased methylations in cellular mRNA 5′ UTRs upon KSHV lytic reactivation, which is in contrast with observations in other viruses such as ZIKV (44). Gene Ontology (GO) term analysis of genes with lytic-specific peaks identified an enrichment for genes with roles in RNA splicing, while genes involved in DNA replication seem to carry less m^{6}A modifications in KSHV lytic cells (Fig. 1*D*). We also detected several m^{6}A peaks within viral genes, many of which have been characterized before (Fig. 1*E* and a complete list of viral peaks position in Table S4) (35, 36, 43). Together, these results reinforce past observations that the m^{6}A profile in lytically infected cells undergoes a massive shift compared to latent cells, redistributing m^{6}A modifications to different host and viral genes, which likely have far-reaching consequences on modulation of gene expression.

IL-6 SRE Carries a Lytic-Specific m^{6}A Modification. We next focused our attention on the IL-6 transcript, the best characterized SOX-resistant mRNA. In latent cells, we detected several m^{6}A peaks between the human genome positions 22,727,199203, which correspond to IL-6 5′ UTR. However, in lytic cells, IL-6 gains an additional peak at position 22,731,646, corresponding to nucleotide 74 on IL-6 3′ UTR. This m^{6}A modification falls on the SRE region and on a strong DRACH motif (Fig. 2*A* and *SI Appendix*, Fig. S3). To confirm the presence of this m^{6}A deposition, we mutated the predicted position within the SRE (referred to as mutSRE) and performed meRIP-qPCR to assess m^{6}A deposition on the WT-SRE (wild-type SRE) compared to the mutSRE. We first verified that our meRIP-qPCR approach on the known m^{6}A-modified transcript DICER (*SI Appendix*, Fig. S1) (22, 36). meRIP-qPCR confirmed the presence of the m^{6}A peak within the SRE and that mutating nucleotide 74 within the IL-6 SRE is enough to abrogate m^{6}A pulldown (Fig. 2*B*).

We next investigated whether this m^{6}A modification plays a role in SRE-mediated escape from SOX-induced decay. Cells were transfected with an SOX construct (or mock) alongside a GFP-expressing reporter bearing no SRE (GFP-∅) and thus susceptible to SOX; a GFP reporter fused to a WTSRE (GFP-WTSRE), expected to be protected from SOX; or fused to mutSRE (GFP-mutSRE) to test the effect of the loss of m^{6}A deposition on escape from SOX. We verified that the levels of relative reporter mRNA levels among the constructs were similar (*SI Appendix*, Fig. S1). As shown in Fig. 2*C*, as expected, SOX efficiently degrades GFP-∅ but GFP-WTSRE resists degradation. However, SOX-mediated decay is restored on the GFP-mutSRE reporter. Since IL-6 is known to also escape decay mediated by closely related SOX homologs, muSOX and BGLF5, we wondered whether the GFP-mutSRE would also be susceptible to these endonucleases. As shown in Fig. 2*C*, a single-point mutation at position 74 in the SRE also renders transcripts susceptible to degradation from SOX homologs. Taken together, these data reveal that m^{6}A modification of the 3′ UTR of IL-6 promotes its escape from SOX.

The m^{6}A Reader YTHDC2 Promotes the SRE Escape from SOX. A previous ChIRP-MS (comprehensive identification of RNA-binding proteins by mass spectrometry) screen had identified a number of host proteins that can bind the SRE element (15). One of these predicted interactors was the m^{6}A reader YTHDC2. Several reports have demonstrated that YTHDC2 directly binds to m^{6}A-modified mRNAs often within 3′ UTRs (45–48). YTHDC2 itself is an RNA helicase and its binding to mRNA has been associated with alteration of RNA stability (45–48). We first confirmed the interaction between YTHDC2 and SRE-bearing mRNA by performing IPs from cells transfected with a GFP reporter fused to the WTSRE (Fig. 3*A*). In agreement with our previous observations, YTHDC2 binding to the m^{6}A-deficient mutSRE was reduced compared to the WTSRE, confirming that YTHDC2 is recruited to the SRE as an m^{6}A reader (Fig. 3*A*).

Since the m^{6}A modification that we identified on the SRE appears to be important to promote protection from SOX-induced degradation, we next asked whether this protective

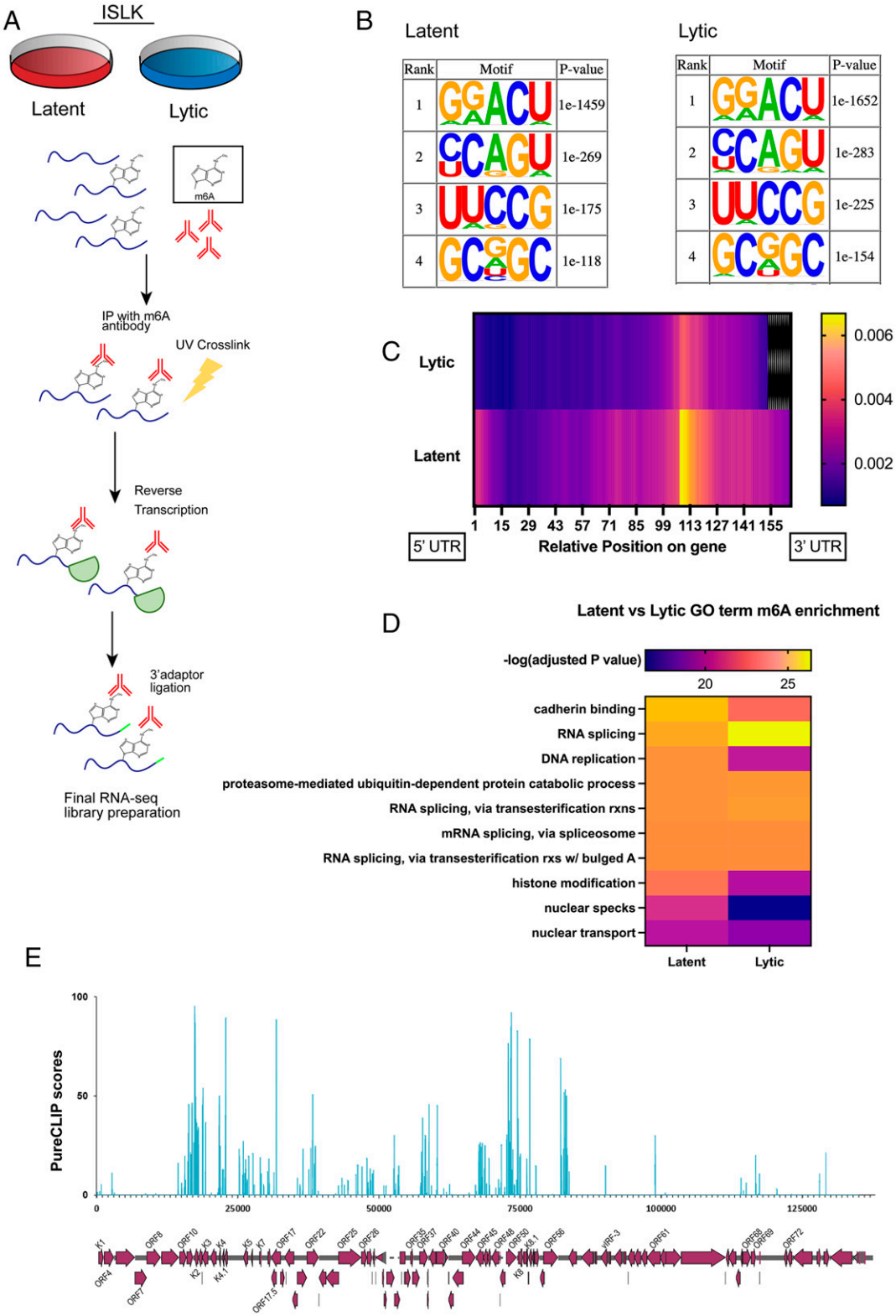

Fig. 1. Examining iSLK m^{6}A epitranscriptome during KSHV lytic reactivation. (*A*) Schematic of m^{6}A eCLIP set up. iSLK.WT cells were either left latent or lytically reactivated with doxycycline and sodium butyrate for 48 h. Total RNA was collected then incubated with an m^{6}A antibody. Samples were ultraviolet cross-linked before being reverse transcribed then attached with 3′ adapters in part of library preparation. Finally, m^{6}A-enriched samples were sequenced. (*B*) Most significant DRACH motifs with m^{6}A peaks identified by HOMER in latent and lytic cells. (*C*) Heat map of a metagene plot depicting the average number of sites mapped to certain genomic regions. The number of sites is calculated for each region of every gene, the lengths of the regions are then normalized, and the average number of sites for a set number of positions along the regions are calculated. (*D*) Heat map of the most significant m^{6}A-enriched functional pathways in latent and lytic cells calculated through an enrichment analysis preformed using the R package clusterProfiler. (*E*) m^{6}A PureCLIP scores of lytically reactivated KSHV genes aligned over an annotated KSHV genome. PureCLIP is the log posterior probability ratio of the m^{6}A cross-link sites over the input samples.

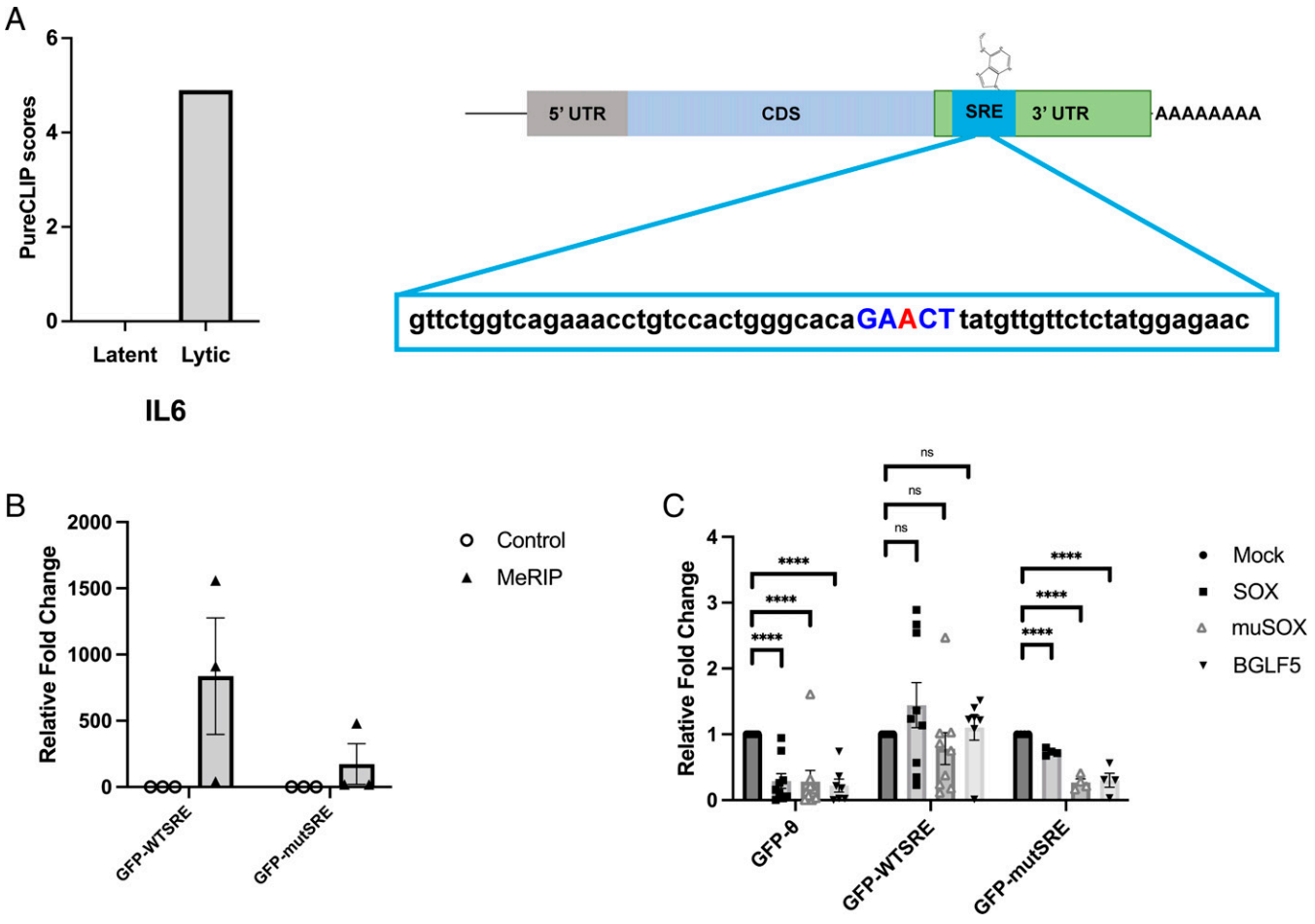

Fig. 2. IL-6 SRE contains an m^{6}A site that is necessary for viral endonuclease protection. (*A*) PureCLIP scores of the 3′ UTR IL-6 gene in latent and lytic (48 hpr) iSLK.WT cells. Schematic to the right illustrates an IL-6 gene (its 5′ UTR, coding region "CDS" and 3′ UTR): the DRACH motif identified through m^{6}A-eCLIP is in blue and the methylated adenosine in red. (*B*) Cells were transfected with WTSRE or mutSRE GFP reporter, and total RNA was harvested 24 h later and subjected to meRIP followed by RT-qPCR using GFP primers. Fold enrichment was determined by calculating the fold change of the IP to control Ct values that were normalized through the input. (*C*) 293T cells transfected with one of three viral endonucleases, as indicated along with the indicated GFP reporters. RNA was collected and quantified using RT-qPCR. ****$P < 0.0001$; ns, not significant.

phenotype was being mediated through the recruitment of YTHDC2. We therefore used Cas9-based genome editing to generate YTHDC2 knockout clones in human embryonic kidney (HEK)293T cells (now referred to as 293TΔYTHDC2). After confirming knockout efficiency (Fig. 3*B*), we used this cell line to assess how the lack of YTHDC2 expression would affect the SRE stability in the face of SOX-mediated decay. 293TΔYTHDC2 were transfected with our GFP-WTSRE reporter along with SOX (or mock), and RNA was extracted and used for RT-qPCR (Fig. 3*C*). As expected, SOX does not affect the RNA levels of the GFP-WTSRE reporter in WT 293T control cells. However, SOX-mediated decay is restored when YTHDC2 expression is knocked down. We observed the same loss of protection on other known SOX escapees like C19ORF66 and GADD45B (*SI Appendix*, Fig. S2). To ensure that this defect in protection from SOX was not due to off-target effects of generating the 293TΔYTHDC2 cell line, we rescued YTHDC2 using ectopic expression (Fig. 3*B*). In these cells, the GFP-WTSRE stability was rescued to normal levels, even in the presence of SOX (Fig. 3*C*). We also investigated the effect of YTHDC2 knockdown in the KSHV-positive iSLK cells. We first investigated the effect of YTHDC2 on proper progression on the viral life cycle and measured the expression of several viral genes upon YTHDC2 knockdown. We also measured the green and red fluorescence of these cells as markers of KSHV latent and lytic phases, respectively. We did not notice any significant changes in the absence of YTHDC2. We, thus, next checked the endogenous levels of several known SOX escapees in the YTHDC2 knockdown cells (*SI Appendix*, Fig. S2). When YTHDC2 expression is knocked down, both C19ORF66 and GADD45b mRNA levels are reduced, indicating that YTHDC2 also modulate their stability in iSLK cells undergoing lytic reactivation and, thus, when SOX exerts its strongest effect on mRNA stability. Taken together, these results support a role for the m^{6}A reader YTHDC2 in protecting transcripts from SOX degradation.

Discussion

Herpesviruses extensively manipulate the fate of host transcripts during lytic reactivation through the use of virally encoded endonucleases. In the case of KSHV, the viral endonuclease SOX targets a wide array of mRNAs via a sequence-specific degron and cleaves around 70% of mRNAs in the cell (1, 49, 50). This allows the virus unfettered access to the host expression machinery for viral replication. Previous work has shown that among the 30% of transcripts that escape this SOX-mediated decay, there is subset of transcripts that carry an RNA stability element located in their 3′ UTR that specifically enables this resistance phenotype against viral but not cellular

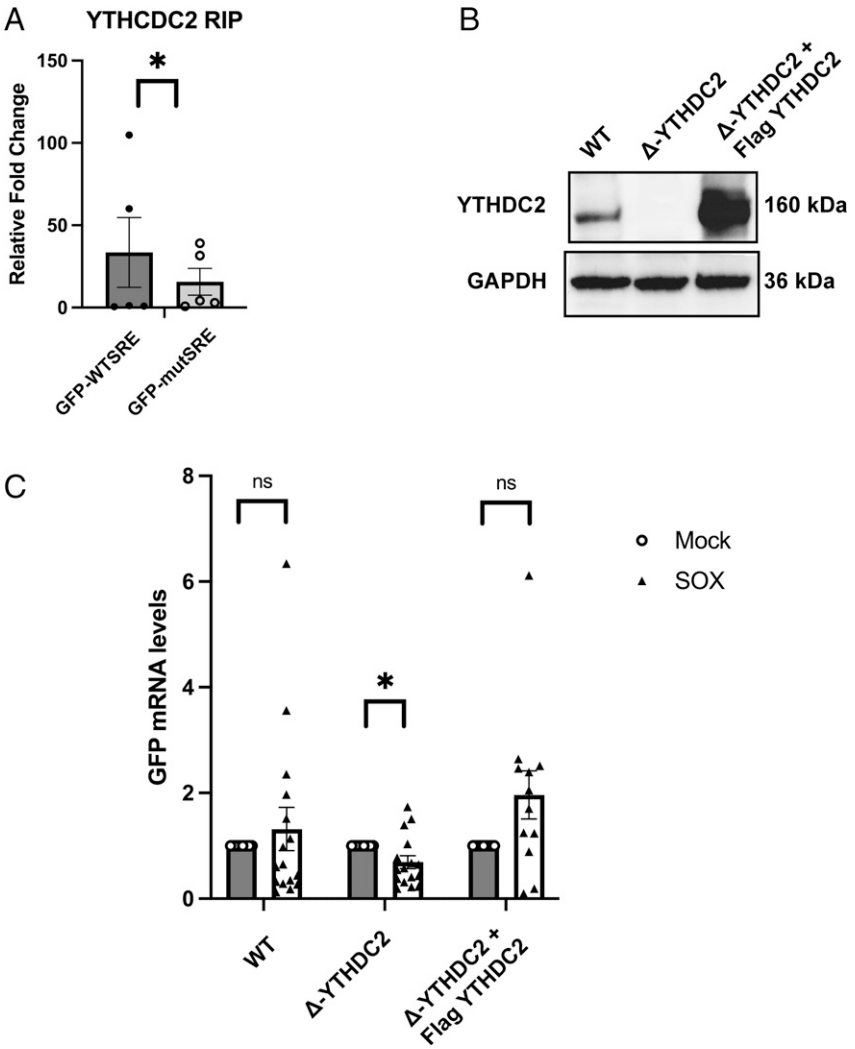

Fig. 3. YTHDC2 is necessary for IL-6's evasion of SOX. (*A*) HEK293T cells were transfected with Flag-tagged YTHDC2 and a GFP-WTSRE reporter as indicated. Cells were cross-linked and IP using Flag-coated beads. RNA fraction was collected and used for RT-qPCR. (*B*) 293TΔYTHDC2 cells were obtained by stably expressing and single-cell–selecting 293TCas9 cells expressing a YTHDC2-targeting guide RNA. Cells' clones were tested for knockout efficiency by Western blot using a YTHDC2 antibody and GAPDH as a loading control. YTHDC2 expression in these cells was rescued by transfecting Flag-tagged YTHDC2 on a plasmid. (*C*) 293TΔYTHDC2, 293TΔYTHDC2+Flag YTHDC2 or WT cells were transfected with SOX (or mock), along with a GFP-WTSRE reporter. RNA was then collected and used for RT-qPCR. *$P < 0.05$; ns, not significant.

endoribonucleases known as the SRE (10, 13–15). While this escape mechanism remains largely uncharacterized, it is known that this RNA element is not conserved in sequence among escaping transcripts but rather adopts a common RNA structure which has been hypothesized to serve as a protein recruitment platform. Past studies have explored proteins bound to this RNA element and found several m^{6}A readers within the SRE RNA–protein complex (15). We thus hypothesized that the RNA modification m^{6}A, which is prevalent and integral to both host and viral transcript fate, may be involved in viral endonuclease escape. This led us to preform m^{6}A-eCLIP sequencing on KSHV latent and lytic cells.

The m^{6}A-eCLIP confirmed previous results seen in which upon reactivation there is an overall decrease in methylation on host transcripts and a massive increase in methylation of viral transcripts (35, 36, 42). Past epitranscriptomic studies exploring KSHV infection had also identified widespread deposition of m^{6}A across the KSHV transcriptome, independently of kinetic classes (35, 36). There is large overlap between the peaks we detected here and these previous studies (Table S4), suggesting that the viral m^{6}A profiles as well as site specificity are conserved. In lytic cells, the pool of mRNA becomes increasingly dominated by viral transcripts; therefore, it is likely that the m^{6}A methyltransferase machinery is more and more solicited and turned toward viral mRNA. In accordance with this possibility, we observed a 5′ UTR hypomethylation and a concomitant 3′ UTR hypermethylation following KSHV reactivation from latency. We know very little about the UTR of KSHV transcripts, but because of genome size constraint, they tend to be much shorter than in average human genes. Therefore, this seemingly preferential 5′ UTR hypomethylation could simply reflect the changes in the pool of mRNA present in the cell at that stage of viral infection. Alternatively, m^{6}A modifications are known to occur mainly cotranscriptionally on the adenosines that are located within a DRACH motif by m^{6}A writer proteins. It is possible that this shift of m^{6}A deposition toward 3′ UTR results from alternative splice forms being expressed during KSHV lytic infection and that, possibly, these transcripts have more favorable DRACH motifs. This can be seen in the shift of the types of transcripts being methylated in Fig. 1*C*. Viruses are known to affect the global gene expression landscape, and it would, thus, not be surprising to see that those expressed

during lytic infection have alternative, 3′ UTR–favoring m^{6}A deposition. This is also in line with our observation that RNA-splicing genes are more m^{6}A modified during the lytic cycle, which could suggest that they are more solicited and possibly more expressed. However, it is still unknown what dictates the m^{6}A-writing machinery to prefer one DRACH motif over another. It is possible that upon lytic reactivation a change occurs in the cell that causes m^{6}A writing to change its "priority." This is supported by a couple of genes like GADD45B and ARMC10, whose m^{6}A transcript landscape shifts during lytic reactivation as well as the DRACH motifs that are methylated (Fig. 1*C*). Interestingly, we know that the m^{6}A deposition on the IL-6 SRE occurs independently of whether this SRE is in the context of the full transcript or simply fused to GFP. Indeed, our results indicated that the presence of the SRE on a GFP reporter is enough to mediate the same "SOX-blocking" effect as in the endogenous mRNA. This suggests that the m^{6}A machinery is likely more influenced by a DRACH motif in the proper context and/or presented in the proper structure than other determinants far away from the DRACH motif chosen. Since m^{6}A is mainly deposited cotranscriptionally perhaps the difference we see in DRACH motif preference is due to transcriptional rate. Another alternative is that, given the increase of RNA splicing, m^{6}A writers preferentially recognize DRACH motifs in actively spliced RNA as a result. Of note, it appears that while pulling down the mutSRE construct was virtually impossible and thus confirming that the SRE only carries one site for methylation, the pulldown for the WTSRE seemed to vary in efficiency. One possibility is that not 100% of the SRE ends up m^{6}A-modified, especially in the context of overexpression of the GFP reporter. It would be interesting to quantify which fraction of the SRE-containing mRNA pool is modified and whether a certain threshold needs to be attained in order to carry the full protection from SOX.

Furthermore, we showed that this reduction in protection extends to SOX homologs muSOX and BGLF5 from MHV68 and EBV, respectively. This would indicate that this m^{6}A "tagging" mechanism may be used widely in the context of infection with gammaherpesviruses to control certain key transcript expression. We also note that, in the context of SOX, there is still some protection of the GFP-mutSRE. SOX's effect on RNA decay is notoriously less prominent than that of its homolog in the closely related other gammaherpesviruses, so this leftover "protection" may be due to SOX's lower efficiency. However, it could also reflect that protection from SOX may rely on more than m^{6}A deposition and need other RNA-binding proteins recruited along the SRE.

We were able to show that the m^{6}A site in the IL-6 SRE recruits YTHDC2 and further demonstrate that the recruitment of this m^{6}A reader is necessary for its protection from SOX. We were also able to see the loss of the protective phenotype for other documented, dominant escapees like C19ORF66 and GADD45B when YTHDC2 was knocked down either in the ΔYTHDC2 or in the iSLK cells. This suggests that the role of YTHDC2 may be conserved among the escapees. It would be interesting to understand both its binding pattern to these mRNAs as well as its role in regulating RNA stability. Moreover, we observed that YTHDC2 depletion does not hinder proper progression of KSHV replication. Interestingly, IL-6 is known to be important for the survival of KSHV-infected cells and play an important role in the establishment of KSHV-associated carcinogenic conversion of infected cells. Therefore, one would predict that affecting IL-6 stability would not have a direct impact on KSHV replication but rather on a global scale and may have an impact on these later stages of infection. It would therefore be interesting to investigate the status of YTHDC2 expression, or lack thereof, in the long-term infection model or in patient tumor samples.

YTHDC2 comes from the YTH family, which boast a YTH binding domain to interact with m^{6}A directly, albeit with low affinity. Interestingly all the other YTH proteins are around 500 to 750 aa and composed of primarily low-complexity disordered regions, while YTHDC2 is close to 1,400 aa in length and has several other known domains besides the canonical YTH domain: an R3H, helicase, ankyrin repeats, HA2, and OB-fold domains (45, 46). Little is known about the function of the canonically cytoplasmic YTHDC2. It has been reported that it may contribute to increased RNA decay by binding select transcripts and XRN1 (46, 47). Other studies have shown that it enhances translation efficiency, unwinding RNA transcripts while bound to the ribosome (45, 51). This puts it in direct contrast with YTHDC1, which is nuclear and has roles in RNA splicing and chromatin modification (52–54). YTHDC2 functions more in line with the cytoplasmic YTHDFs 1 to 3, which have been shown to bind m^{6}A-containing transcripts and enhance translational activity or mRNA decay (55–58). What many of the YTH proteins have in common when binding their transcripts is that they function in complex with other proteins. This is consistent with our hypothesis that although YTHDC2 is necessary for the protection of IL-6 from SOX-mediated decay, it is most likely not sufficient. A previous study has shown that IL-6 binds with nucleolin, HuR, and AUF-1 in a protective complex (10, 14, 15). It is likely that YTHDC2 works in concert with these proteins and possibly others to either occlude SOX targeting via their presence or by relocalizing the transcript where SOX cannot target IL-6. There is also a possibility that the YTHDC2 helicase function may be necessary for protection, and perhaps, the unwinding of the IL-6 transcript removes an internal mRNA secondary structure that is essential for SOX targeting. YTHDC2 binding to the SRE may also extend beyond the m^{6}A requirement. We previously looked into the secondary structure of these SRE and showed that the SRE fold is the most conserved feature of all escaping transcripts, even beyond sequence conservation. By playing with the dynamism of m^{6}A deposition, the structure of the SRE may be modified and therefore impact recruitment of proteins more globally (15). In particular, it would be interesting to investigate the extent of the YTHDC2-binding target to understand whether protection from SOX is more reliant on the presence of YTHDC2 or presence of an m^{6}A modification. Investigating the secondary structure of the WT-SRE versus the mutant SRE could also reveal how the presence of this modification influences hairpin formation. Recent studies have shown that m^{6}A can influence the formation of double-stranded (ds) RNA and that, during viral infection, this could help prevent detection by dsRNA sensor–like RIG-I (retinoic acid-inducible gene I)(59, 60). Therefore, one can anticipate that m^{6}A deposition on the SRE could similarly influence RNA fate.

Furthermore, while our data supports the role of m^{6}A as an important contributor to SOX resistance, it also emerges that this is not the sole answer of SRE protection. We did not find a consistent pattern in lytic-specific m^{6}A deposition in other known or predicted, SOX-resistant transcripts. These escaping mRNAs either had no change in their m^{6}A status upon lytic infection or had lytic-specific peaks outside of their 3′ UTR. This indicates that it is not lytic infection per se that triggers this escape phenotype and/or directs m^{6}A deposition but rather that some m^{6}A-modified mRNAs are compatible with assembling a protective complex against SOX. Therefore, not all m^{6}A transcripts turn out to be SOX resistant, which is in line with our observations that only select transcripts among the 20% spared from SOX decay are actively escaping degradation. We thus hypothesize that these m^{6}A modifications must be in the proper context and recruit a specific set of protective proteins in order to be active. However, now that we have a clearer idea of what m^{6}A reader may be involved in this mechanism, it

would be interesting to reverse our question and search for new escapees using either their m^{6}A pattern and/or by investigating what transcripts are bound by YTHDC2 during KSHV lytic infection. Furthermore, given that the regulation of RNA fate is a crucial step in hijacking the host cell, it is perhaps unsurprising that several viruses use widespread RNA decay to take over their hosts. It would be interesting to investigate the contribution of m^{6}A modifications and the YTHDC2 role in these other viral families that also deploy host shutoff as a way to overtake the host.

Materials and Methods

Cells and Transfections. HEK293T 293 cells (ATCC) were grown in Dulbecco's modified Eagle's medium (DMEM; Invitrogen) supplemented with 10% fetal bovine serum (FBS). The KSHV-infected renal carcinoma human cell line iSLK.219 (cells were supplied by Britt Glaunsinger, UC Berkeley, CA)[close space]-bearing, doxycycline-inducible RTA was grown in DMEM supplemented with 10% FBS (61). Lytic reactivation cells were induced by the addition of 0.2 μg/mL doxycycline (BD Biosciences) and 110 μg/mL sodium butyrate for 72 h. The 293TΔYTHDC2 knockout clone and control Cas9-expressing cells were made by transducing HEK293T cells, as previously described (62, 63). Briefly, lenti-Cas9-blast lentivirus was spinfected onto a monolayer of HEK293T cells, which were then incubated with 20 μg/mL blasticidin for a selection of transduced cells. These HEK293T-Cas9 cells were then spinfected with lentivirus made from pLKO-tet on containing the YTHDC2 sgRNA (single guide RNA) sequence, designed using the broad institute analysis tool and checked for off-target effects. After selection using and 1 μg/mL puromycin, the pool of YTHDC2 knockout cells was then single-cell cloned in 96-well plates, and individual clones were screened by Western blot to determine knockout efficiency.

For DNA transfections, cells were plated and transfected after 24 h when 70% confluent using PolyJet (SignaGen).

Plasmids. The GFP-based reporters and SOX expression plasmids were described previously (15). The mutSRE reporter was generated by introducing an A to T point mutation at position 74 of the WTSRE using the Quickchange site-directed mutagenesis protocol (Agilent) using the primers described in Table S1. YTHDC2 expression plasmid was supplied by Chuan He, University of Chicago, IL.

RT-qPCR. Total RNA was harvested using TRIzol according to the manufacturer's protocol. cDNAs (complementary DNA) were synthesized from 1 μg total RNA using avian myeloblastosis virus (AMV) reverse transcriptase (Promega) and used directly for qPCR analysis with the SYBR green qPCR kit (Bio-Rad). Ct values (cycle thresholds) signals obtained by qPCR were normalized to those for 18S unless otherwise noted.

Western Blotting. Cell lysates were prepared in lysis buffer (NaCl, 150 mM; Tris, 50 mM; Nonidet P-40, 0.5%; dithiothreitol [DTT], 1 mM; and protease inhibitor tablets) and quantified by Bradford assay. Equivalent amounts of each sample were resolved by SDS-PAGE and Western blotted with the following antibodies at 1:1,000 in Tris-buffered saline, 0.1% Tween 20, rabbit anti-YTHDC2 (Abcam), and mouse anti-GAPDH (Abcam). Primary antibody incubations were followed by horseradish peroxidase–conjugated goat anti-mouse or goat anti-rabbit secondary antibodies (1:5,000; Southern Biotechnology).

meRIP-qPCR. HEK293T or iSLK cells were transfected as indicated and used for meRIP (methylated [m^{6}A] RNA immunoprecipitation); then, total RNA was extracted using TRIzol. Pulldowns were performed using protein G Dynabeads (Invitrogen) with 10 μg m^{6}A antibody (Sigma-Aldrich) and 100 μg RNA in meRIP buffer (50 mM Tris·HCl at 7.4 pH,150 mM NaCl, 1 mM EDTA, 0.1% Nonidet P-40, Millipore H_2O) and 1 μL RNAsin (RNAse inhibitor - Promega) per sample overnight at 4 °C. After extensive washing, samples are eluted in meRIP buffer containing 6.7 mM sodium salt for 30 min at 4 °C. cDNAs were then obtained from 1 μg total RNA using AMV reverse transcriptase (Promega) and used directly for qPCR analysis with the SYBR green qPCR kit (Bio-Rad).

RIP. Cells were cross-linked in 1% formaldehyde for 10 min, quenched in 125 mM glycine, and washed in PBS (phosphate buffered saline). Cells were then lysed in low-salt lysis buffer (NaCl 150 mM, Nonidet P-40 0.5%, Tris pH 8 50 mM, DTT 1 mM, MgCl2 3 mM containing protease inhibitor mixture and RNase inhibitor) and sonicated. After removal of cell debris, specific antibodies were added as indicated overnight at 4 °C. Magnetic, G-coupled beads were added for 1 h and washed three times with lysis buffer and twice with high-salt lysis buffer (low-salt lysis buffer except containing 400 mM NaCl). Samples were separated into two fractions. Beads containing the fraction used for Western blotting were resuspended in 30 μL lysis buffer. Beads containing the fraction used for RNA extraction were resuspended in proteinase K (PK) buffer (NaCl 100 mM, Tris pH 7.4 10 mM, EDTA 1 mM, SDS 0.5%) containing 1 μL PK. Samples were incubated overnight at 65 °C to reverse cross-linking. Samples to be analyzed by Western blot were then supplemented with 10 μL 4× loading buffer before resolution by SDS-PAGE (sodium dodecyl sulphate–polyacrylamide gel electrophoresis). RNA samples were resuspended in TRIzol and were processed as described in *RT-qPCR*.

eCLIP and RNA-seq. iSLK.219 cells were harvested in their latent phase or 48-h postreactivation. RNA was then extracted by TRIzol and purified as described in *RT-qPCR*. The samples were processed by EclipseBio as described in their user guide, performing 150 paired-end run on NovaSeq6000 on was PolyA-selected RNA. Ratio of IP and input reads were evaluated in each cluster, and clusters with IP/input enrichment greater than eightfold and associated P value < 0.001 were defined as significant "peaks." PureCLIP was used to identify m^{6}A sites with a single-nucleotide resolution. This algorithm identifies cross-link sites in eCLIP experiments and assesses enrichment of DRACH motif relative to reads starts in IP and input libraries, as well as what fraction of identified cross-link sites are positioned on DRACH motifs.

Statistical Analysis. All results are expressed as means ± SEMs of experiments independently repeated at least three times (individual replicate points are shown on bar graph). The unpaired Student's t test was used to evaluate the statistical difference between samples. Significance was evaluated with P values as follows: *P < 0.05; **P < 0.01; ***P < 0.001; ****P < 0.0001; and ns refers to not significant.

Data Availability. Sequencing file data have been deposited in National Center for Biotechnology Information Gene Expression Omnibus (GSE194100). All other study data are included in the article and/or supporting information.

ACKNOWLEDGMENTS. We thank all members of the Muller laboratory for helpful discussions and suggestions. We are grateful to Dr. Chuan He for the YTHDC2-expressing plasmid and Britt Glaunsinger for cells and antibodies. We also thank Eclipse Bio for their support. This research was supported by University of Massachusetts, Amherst Microbiology Startup funds and NIH Grant R35GM138043 (to M.M.), a Spaulding Smith fellowship (to D.M.-F.), and the BioEclipse RNA award (to D.M.-F.).

1. H. Lee *et al.*, KSHV SOX mediated host shutoff: The molecular mechanism underlying mRNA transcript processing. *Nucleic Acids Res.* **45**, 4756–4767 (2017).
2. B. Glaunsinger, D. Ganem, Lytic KSHV infection inhibits host gene expression by accelerating global mRNA turnover. *Mol. Cell* **13**, 713–723 (2004).
3. M. Rowe *et al.*, Host shutoff during productive Epstein-Barr virus infection is mediated by BGLF5 and may contribute to immune evasion. *Proc. Natl. Acad. Sci. U.S.A.* **104**, 3366–3371 (2007).
4. S. Covarrubias, J. M. Richner, K. Clyde, Y. J. Lee, B. A. Glaunsinger, Host shutoff is a conserved phenotype of gammaherpesvirus infection and is orchestrated exclusively from the cytoplasm. *J. Virol.* **83**, 9554–9566 (2009).
5. J. M. Richner *et al.*, Global mRNA degradation during lytic gammaherpesvirus infection contributes to establishment of viral latency. *PLoS Pathog.* **7**, e1002150 (2011).
6. E. Abernathy *et al.*, Gammaherpesviral gene expression and virion composition are broadly controlled by accelerated mRNA degradation. *PLoS Pathog.* **10**, e1003882 (2014).
7. M. M. Gaglia, C. H. Rycroft, B. A. Glaunsinger, Transcriptome-wide cleavage site mapping on cellular mRNAs reveals features underlying sequence-specific cleavage by the viral ribonuclease SOX. *PLoS Pathog.* **11**, e1005305 (2015).
8. A. S. Mendez, C. Vogt, J. Bohne, B. A. Glaunsinger, Site specific target binding controls RNA cleavage efficiency by the Kaposi's sarcoma-associated herpesvirus endonuclease SOX. *Nucleic Acids Res.* **46**, 11968–11979 (2018).
9. S. Covarrubias *et al.*, Coordinated destruction of cellular messages in translation complexes by the gammaherpesvirus host shutoff factor and the mammalian exonuclease Xrn1. *PLoS Pathog.* **7**, e1002339 (2011).
10. S. Hutin, Y. Lee, B. A. Glaunsinger, An RNA element in human interleukin 6 confers escape from degradation by the gammaherpesvirus SOX protein. *J. Virol.* **87**, 4672–4682 (2013).
11. K. Clyde, B. A. Glaunsinger, "Getting the message: Direct manipulation of host mRNA accumulation during gammaherpesvirus lytic infection" in *Advances in Virus Research*, K. Maramorosch, A. J. Shatkin, F. A. Murphy, Eds. (Academic Press, 2010), pp. 1–42.
12. S. Chandriani, D. Ganem, Host transcript accumulation during lytic KSHV infection reveals several classes of host responses. *PLoS One* **2**, e811 (2007).
13. K. Clyde, B. A. Glaunsinger, Deep sequencing reveals direct targets of gammaherpesvirus-induced mRNA decay and suggests that multiple mechanisms govern cellular transcript escape. *PLoS One* **6**, e19655 (2011).

14. M. Muller *et al.*, A ribonucleoprotein complex protects the interleukin-6 mRNA from degradation by distinct herpesviral endonucleases. *PLoS Pathog.* **11**, e1004899 (2015).
15. M. Muller, B. A. Glaunsinger, Nuclease escape elements protect messenger RNA against cleavage by multiple viral endonucleases. *PLoS Pathog.* **13**, e1006593 (2017).
16. W. Rodriguez, K. Srivastav, M. Muller, C19ORF66 broadly escapes virus-induced endonuclease cleavage and restricts Kaposi's sarcoma-associated herpesvirus. *J. Virol.* **93**, e00373-19 (2019).
17. B. Glaunsinger, D. Ganem, Highly selective escape from KSHV-mediated host mRNA shutoff and its implications for viral pathogenesis. *J. Exp. Med.* **200**, 391–398 (2004).
18. R. Desrosiers, K. Friderici, F. Rottman, Identification of methylated nucleosides in messenger RNA from Novikoff hepatoma cells. *Proc. Natl. Acad. Sci. U.S.A.* **71**, 3971–3975 (1974).
19. W. Wei, X. Ji, X. Guo, S. Ji, Regulatory role of N^6-methyladenosine (m^6A) methylation in RNA processing and human diseases. *J. Cell. Biochem.* **118**, 2534–2543 (2017).
20. K. D. Meyer *et al.*, Comprehensive analysis of mRNA methylation reveals enrichment in 3′ UTRs and near stop codons. *Cell* **149**, 1635–1646 (2012).
21. S. Ke *et al.*, A majority of m6A residues are in the last exons, allowing the potential for 3′ UTR regulation. *Genes Dev.* **29**, 2037–2053 (2015).
22. D. Dominissini *et al.*, Topology of the human and mouse m6A RNA methylomes revealed by m6A-seq. *Nature* **485**, 201–206 (2012).
23. P. J. Batista *et al.*, m(6)A RNA modification controls cell fate transition in mammalian embryonic stem cells. *Cell Stem Cell* **15**, 707–719 (2014).
24. M. Lee, B. Kim, V. N. Kim, Emerging roles of RNA modification: m(6)A and U-tail. *Cell* **158**, 980–987 (2014).
25. T. Chen *et al.*, m(6)A RNA methylation is regulated by microRNAs and promotes reprogramming to pluripotency. *Cell Stem Cell* **16**, 289–301 (2015). Correction in: *Cell Stem Cell* **16**, 338 (2015).
26. X.-L. Ping *et al.*, Mammalian WTAP is a regulatory subunit of the RNA N6-methyladenosine methyltransferase. *Cell Res.* **24**, 177–189 (2014).
27. Y. Wang *et al.*, N6-methyladenosine modification destabilizes developmental regulators in embryonic stem cells. *Nat. Cell Biol.* **16**, 191–198 (2014).
28. J. Liu *et al.*, A METTL3-METTL14 complex mediates mammalian nuclear RNA N6-adenosine methylation. *Nat. Chem. Biol.* **10**, 93–95 (2014).
29. J. A. Bokar, M. E. Shambaugh, D. Polayes, A. G. Matera, F. M. Rottman, Purification and cDNA cloning of the AdoMet-binding subunit of the human mRNA (N6-adenosine)-methyltransferase. *RNA* **3**, 1233–1247 (1997).
30. F. Ye, RNA N^6-adenosine methylation (m^6A) steers epitranscriptomic control of herpesvirus replication. *Inflamm. Cell Signal.* **4**, e1604 (2017).
31. S. Zaccara, R. J. Ries, S. R. Jaffrey, Reading, writing and erasing mRNA methylation. *Nat. Rev. Mol. Cell Biol.* **20**, 608–624 (2019).
32. G. Zheng *et al.*, ALKBH5 is a mammalian RNA demethylase that impacts RNA metabolism and mouse fertility. *Mol. Cell* **49**, 18–29 (2013).
33. G. Jia *et al.*, N6-methyladenosine in nuclear RNA is a major substrate of the obesity-associated FTO. *Nat. Chem. Biol.* **7**, 885–887 (2011). Correction in: *Nat. Chem. Biol.* **8**, 1008 (2012).
34. B. Slobodin *et al.*, Transcription impacts the efficiency of mRNA translation via co-transcriptional N6-adenosine methylation. *Cell* **169**, 326–337.e12 (2017).
35. B. Tan *et al.*, Viral and cellular N 6-methyladenosine and N 6, 2′-O-dimethyladenosine epitranscriptomes in the KSHV life cycle. *Nat. Microbiol.* **3**, 108–120 (2018).
36. C. R. Hesser, J. Karijolich, D. Dominissini, C. He, B. A. Glaunsinger, N6-methyladenosine modification and the YTHDF2 reader protein play cell type specific roles in lytic viral gene expression during Kaposi's sarcoma-associated herpesvirus infection. *PLoS Pathog.* **14**, e1006995 (2018).
37. N. S. Gokhale *et al.*, N6-methyladenosine in Flaviviridae viral RNA genomes regulates infection. *Cell Host Microbe* **20**, 654–665 (2016).
38. E. M. Kennedy *et al.*, Posttranscriptional m^6A editing of HIV-1 mRNAs enhances viral gene expression. *Cell Host Microbe* **19**, 675–685 (2016). Correction in: *Cell Host Microbe* **22**, 830 (2017).
39. G. D. Williams, N. S. Gokhale, S. M. Horner, Regulation of viral infection by the RNA modification N6-methyladenosine. *Annu. Rev. Virol.* **6**, 235–253 (2019).
40. A. B. R. Mcintyre *et al.*, Altered m^6A modification of specific cellular transcripts affects Flaviviridae infection. *Mol. Cell* **77**, 542–555.e8 (2020).
41. F. Ye, E. R. Chen, T. W. Nilsen, Kaposi's sarcoma-associated herpesvirus utilizes and manipulates RNA N^6-adenosine methylation to promote lytic replication. *J. Virol.* **91**, e00466-17 (2017).
42. S. E. Martin, H. Gan, G. Toomer, N. Sridhar, J. Sztuba-Solinska, The m^6A landscape of polyadenylated nuclear (PAN) RNA and its related methylome in the context of KSHV replication. *RNA* **27**, 1102–1125 (2021). Correction in: *RNA* **28**, 274 (2022).
43. F. Ye, RNA N^6-adenosine methylation (m^6A) steers epitranscriptomic control of herpesvirus replication. *Inflamm. Cell Signal.* **4**, e1604 (2017).
44. G. Lichinchi *et al.*, Dynamics of human and viral RNA methylation during Zika virus infection. *Cell Host Microbe* **20**, 666–673 (2016).
45. P. J. Hsu *et al.*, Ythdc2 is an N 6-methyladenosine binding protein that regulates mammalian spermatogenesis. *Cell Res.* **27**, 1115–1127 (2017).
46. M. N. Wojtas *et al.*, Regulation of m6A transcripts by the 3→5 RNA helicase YTHDC2 is essential for a successful meiotic program in the mammalian germline. *Mol. Cell* **68**, 374–387.e12 (2017).
47. J. Kretschmer *et al.*, The m6A reader protein YTHDC2 interacts with the small ribosomal subunit and the 5′-3′ exoribonuclease XRN1. *RNA* **24**, 1339–1350 (2018).
48. C. Ma, S. Liao, Z. Zhu, Crystal structure of human YTHDC2 YTH domain. *Biochem. Biophys. Res. Commun.* **518**, 678–684 (2019).
49. T. He *et al.*, Host shutoff activity of VHS and SOX-like proteins: Role in viral survival and immune evasion. *Virol. J.* **17**, 68 (2020).
50. B. Glaunsinger, L. Chavez, D. Ganem, The exonuclease and host shutoff functions of the SOX protein of Kaposi's sarcoma-associated herpesvirus are genetically separable. *J. Virol.* **79**, 7396–7401 (2005).
51. Y. Mao *et al.*, m6A in mRNA coding regions promotes translation via the RNA helicase-containing YTHDC2. *Nat. Commun.* **10**, 5332 (2019).
52. D. Zhen *et al.*, m^6A reader: Epitranscriptome target prediction and functional characterization of N6-methyladenosine (m^6A) readers. *Front. Cell Dev. Biol.* **8**, 741 (2020).
53. G.-W. Kim, H. Imam, A. Siddiqui, The RNA binding proteins YTHDC1 and FMRP regulate the nuclear export of N6-methyladenosine modified Hepatitis B Virus transcripts and affect the viral life cycle. *J. Virol.* **95**, e0009721 (2021).
54. W. Xiao *et al.*, Nuclear m(6)A reader YTHDC1 regulates mRNA splicing. *Mol. Cell* **61**, 507–519 (2016). Correction in: *Mol. Cell* **61**, 925 (2016).
55. Y. Fu, X. Zhuang, m^6A-binding YTHDF proteins promote stress granule formation. *Nat. Chem. Biol.* **16**, 955–963 (2020).
56. X.-Y. Chen *et al.*, The m^6A reader YTHDF1 facilitates the tumorigenesis and metastasis of gastric cancer via USP14 translation in an m^6A-dependent manner. *Front. Cell Dev. Biol.* **9**, 647702 (2021).
57. H. Shi *et al.*, YTHDF3 facilitates translation and decay of N^6-methyladenosine-modified RNA. *Cell Res.* **27**, 315–328 (2017).
58. Y. Zhang *et al.*, RNA-binding protein YTHDF3 suppresses interferon-dependent antiviral responses by promoting FOXO3 translation. *Proc. Natl. Acad. Sci. U.S.A.* **116**, 976–981 (2019).
59. N. Li *et al.*, METTL3 regulates viral m6A RNA modification and host cell innate immune responses during SARS-CoV-2 infection. *Cell Rep.* **35**, 109091 (2021).
60. Y. Gao *et al.*, m^6A modification prevents formation of endogenous double-stranded RNAs and deleterious innate immune responses during hematopoietic development. *Immunity* **52**, 1007–1021.e8 (2020).
61. J. Myoung, D. Ganem, Generation of a doxycycline-inducible KSHV producer cell line of endothelial origin: Maintenance of tight latency with efficient reactivation upon induction. *J. Virol. Methods* **174**, 12–21 (2011).
62. N. E. Sanjana, O. Shalem, F. Zhang, Improved vectors and genome-wide libraries for CRISPR screening. *Nat. Methods* **11**, 783–784 (2014).
63. O. Shalem *et al.*, Genome-scale CRISPR-Cas9 knockout screening in human cells. *Science* **343**, 84–87 (2014).